Uncoupling the TFIIH Core and Kinase Modules Leads To Misregulated RNA Polymerase II CTD Serine 5 Phosphorylation

Gabriela Giordano[1], Robin Buratowski[1], Célia Jeronimo[2], Christian Poitras[2]
François Robert[2,3,4], and Stephen Buratowski[1,*]

[1]Department of Biological Chemistry and Molecular Pharmacology,
Harvard Medical School, Boston, MA.

[2]Institut de recherches cliniques de Montréal (IRCM),
Montréal, Québec, Canada

[3]Département de Médecine, Université de Montréal, Montréal, Québec, Canada

[4]Division of Experimental Medicine, Medicine, McGill University, Montréal, Québec, Canada

*Corresponding Author:
steveb@hms.harvard.edu
1-617-432-0696

Classification: Biological Sciences: Biochemistry, Genetics

Abstract

TFIIH is an essential transcription initiation factor for RNA polymerase II (RNApII). This multi-subunit complex comprises two modules that are physically linked by the subunit Tfb3 (MAT1 in metazoans). The TFIIH Core Module, with two DNA-dependent ATPases and several additional subunits, promotes DNA unwinding. The TFIIH Kinase Module phosphorylates Serine 5 of the C-terminal domain (CTD) of RNApII subunit Rpb1, a modification that coordinates exchange of initiation and early elongation factors. While it is not obvious why these two disparate activities are bundled into one factor, the connection may provide temporal coordination during early initiation. Here we show that Tfb3 can be split into two parts to uncouple the TFIIH modules. The resulting cells grow slower than normal, but are viable. Chromatin immunoprecipitation of the split TFIIH shows that the Core Module, but not the Kinase, is properly recruited to promoters. Instead of the normal promoter-proximal peak, high CTD Serine 5 phosphorylation is seen throughout transcribed regions. Therefore, coupling the TFIIH modules is necessary to localize and limit CTD kinase activity to early stages of transcription. These results are consistent with the idea that the two TFIIH modules began as independent functional entities that became connected by Tfb3 during early eukaryotic evolution.

Significance Statement: The RNA polymerase II initiation factor TFIIH provides two activities needed for efficient transcription: promoter unwinding and phosphorylation of polymerase subunit Rpb1 on its C-terminal domain (CTD). This study shows these two functions can be physically uncoupled. Unexpectedly, when the CTD kinase is no longer recruited to the promoter, the CTD phosphorylation on Serine 5 is not lost, but instead occurs throughout transcription. These results suggest that fusion of the two TFIIH activities evolved to better target CTD Serine 5 phosphorylation to early elongation.

INTRODUCTION

The three nuclear RNA polymerases in eukaryotes share many features, reflecting their evolution from a single precursor (reviewed in (1)). Their multiple subunits are either homologous or identical, and the initiation factors needed to direct all three polymerases to their appropriate target promoters include both the TATA-Binding Protein (TBP) and a TFIIB-like factor. Extending the parallels, RNA polymerases I and III contain intrinsic subunits that resemble the RNA polymerase II (RNApII) initiation factors TFIIE or TFIIF, which help direct the template DNA into the active site cleft.

In contrast to this overall mechanistic conservation, RNApII initiation factor TFIIH has no obvious counterparts in the other polymerase systems. Accordingly, TFIIH performs two functions that are unique to RNApII (2). The first is the use of ATP hydrolysis to accelerate promoter melting, and the second is phosphorylation of a unique C-terminal domain (CTD) on Rpb1, the largest RNApII subunit. These two activities presumably evolved after the divergence of the three RNA polymerases.

The two TFIIH functions map to distinct sub-complexes, sometimes called modules, that are apparent in the TFIIH structure (**Fig. 1A**). Ssl2 (XPB in metazoans) is the DNA-dependent ATPase that pushes double-stranded DNA towards the RNApII active site, leading to strand separation and placement of the template strand in the polymerase active site (3). Ssl2/XPB interacts with DNA downstream of RNApII, held in place by six other subunits (Tfb1, Tfb2, Tfb4, Tfb5, Rad3/XPD, and Ssl1) that make up the "Core" TFIIH subcomplex. TFIIH binding to the pre-initiation complex (PIC) is mediated by interactions of the Core with TFIIE and the Rpb4/7 stalk of RNApII (4-6). It is not obvious why so many TFIIH subunits should be necessary for the promoter melting function. Interestingly, the Rad3 (XPD in metazoans) subunit is also a DNA-dependent ATPase, but it translocates along DNA in the opposite direction to Ssl2/XPB. Surprisingly, Rad3 makes no contact with DNA in PIC structures, and catalytically inactive Rad3 mutants do not affect transcription (7, 8). The apparent explanation for the existence of the "extra" subunits and functions in the TFIIH Core is that it also functions as a DNA nucleotide excision repair (NER) enzyme. In that process, both ATPases unwind DNA to expose a short stretch of the damaged strand for removal (9-11). It therefore seems most likely that the TFIIH Core module originally evolved for DNA repair, and only later was co-opted for RNApII transcription.

The second TFIIH sub-complex carries the CTD phosphorylation activity. The kinase Kin28 (CDK7 in metazoans) and its cyclin partner Ccl1 (Cyclin H) phosphorylate CTD Serine 5. PIC structures show that the Mediator complex helps guide the CTD to the kinase module (4, 5, 12, 13). CTD phosphorylation triggers release of Mediator, as well as subsequent recruitment of mRNA capping enzyme and other factors that function near 5' ends of mRNAs (reviewed in (14)). Like the Core, the Kinase module also has a second function unrelated to transcription. At least in metazoans, CDK7/cyclin H serves as a CDK-activating kinase (CAK), phosphorylating the T-loop of other cyclin-dependent kinases to promote an active conformation (15). This is not a universal function, as *Saccharomyces cerevisiae* and some other species have a separate CAK enzyme (16-18). Nonetheless, it seems likely that the activity of CDK7 on RNApII evolved from a pre-existing CDK that had either CAK activity or some other function.

The two TFIIH subcomplexes are linked by the Tfb3 subunit (known as MAT1 in metazoans). Tfb3/MAT1 consists of two globular domains and a linker region. The N-terminal

104 domain is part of the Core module, where it helps incorporate TFIIH into the PIC through direct
105 interactions with RNApII and TFIIE (13). The Tfb3 C-terminal domain contacts both the kinase
106 and cyclin subunits, and this interaction promotes an active kinase conformation (19-21). PIC
107 structures show the linker emerging from the N-terminal domain as a long alpha-helix running
108 along the interface between the two ATPase subunits, followed by a turn and a short stretch of
109 helix just N-terminal to a disordered region that connects to the C-terminal region (see
110 schematic in **Fig. 1A**). A deletion study in yeast showed that Tfb3 tolerates 30 amino acid
111 deletions throughout the linker, but that the N- and C-terminal domains were essential for
112 viability (22).
113 Given its modular structure, we tested whether other CTD kinases could be fused to
114 Tfb3 to bypass the requirement for Kin28/CDK7. While the results have so far been negative,
115 we unexpectedly found that cells lacking the C-terminal domain of Tfb3 were actually viable,
116 albeit very slow growing. Remarkably, growth is significantly rescued when the two parts of
117 Tfb3 are expressed as separate proteins. In these cells, the TFIIH kinase module is no longer
118 tethered to the Core TFIIH. ChIP experiments show that the Core Module, but not the Kinase, is
119 still promoter localized. Surprisingly, phosphorylation of CTD Serine 5 is now seen at higher
120 than normal levels throughout transcribed regions, indicating that the untethered kinase
121 accesses RNApII throughout the cell cycle. These results are consistent with the idea that the
122 two TFIIH modules began as independent entities that only later became fused into a single
123 complex.
124
125
126

127 **RESULTS**

128 **Tethering other kinase modules to Tfb3 does not bypass the requirement for Kin28.**
129 Given the apparent modularity of TFIIH, we asked whether tethering other kinases to Tfb3
130 could functionally replace Kin28. Although Kin28 phosphorylates CTD Serine 5 in vivo, other
131 kinases can phosphorylate this residue in vitro. Two other transcription kinase complexes,
132 Bur1/Bur2 (the yeast homologs of CDK9/cyclin T) and Ctk1/Ctk2/Ctk3 (yeast CDK12/Cyclin K),
133 phosphorylate the Rpb1 linker (23) and CTD Serine 2 (24), respectively. However, both are
134 reported to also have activity on Serine 5, at least in vitro (25-27). Accordingly, we constructed
135 Tfb3 fusions **(Fig. 1B, Supplemental Table 1)** in which the C-terminal region was replaced with
136 either Bur2 (the cyclin partner of Bur1) or Ctk3 (the third subunit within the Ctk1/Ctk2
137 CDK/cyclin complex). We also created a fusion of the Tfb3 N-terminal domain and linker to
138 Mpk1, a single subunit kinase also reported to have activity on CTD Serine 5, as well as Ser2 and
139 Tyr1 (28).

140 The three fusion constructs were introduced into a yeast strain lacking the chromosomal
141 copy of *KIN28*. Expression of the fusion proteins was confirmed by immunoblotting
142 (**Supplemental Fig. S1**). None of the fusions supported viability after plasmid shuffling to
143 remove *KIN28* (**Fig. 1C**), indicating that tethering the other kinases could not substitute for
144 Kin28 function. As a control experiment, the Tfb3 fusions were also tested for complementation
145 of a *TFB3* deletion. Surprisingly, these shuffled strains proved to be viable, albeit so slow
146 growing that 5-7 days were needed to see colonies **(Fig. 1D)**. Complementation of *tfb3*Δ
147 indicates that the fusion proteins were incorporated into TFIIH. This result was unexpected
148 because a *TFB3* allele encoding amino acids 1-275, and therefore lacking the C-terminal
149 domain, did not support growth, consistent with earlier reports that the C-terminal domain is
150 essential for Tfb3 function and cell viability (22, 29).

151 **The N-terminal domain is the only essential part of Tfb3.** The unexpected
152 complementation of *tfb3*Δ by the Tfb3 fusions raised the question of whether the Tfb3 C-
153 terminal domain was truly essential for viability. Earlier studies may not have waited long
154 enough to see growth. Also, the restriction fragment deletion used to create the non-
155 complementing Tfb3(1-275) allele used in **Figure 1D** also removed the 3' untranslated region
156 and polyA site (29), which could further impair function beyond the loss of the C-terminal
157 domain. Accordingly, we created a new set of Tfb3 truncations, each lacking either one or two
158 of the three major Tfb3 domains **(Fig. 2A)**, and used plasmid shuffling to introduce them into a
159 *tfb3*Δ strain. Cells lacking the N-terminal domain failed to grow, no matter how long the plates
160 were incubated **(Fig. 2B**). In contrast, strains expressing only the N-terminal (N-term) domain,
161 or the N-terminal and Linker (N-term-Linker) domains, exhibited slow growth. These deletions
162 grew at rates similar to the fusion proteins tested above, arguing that the fused kinase module
163 did not provide an additional function or stability relative to a Tfb3 completely lacking any
164 sequence C-terminal to the Linker region. We therefore conclude that, while important for
165 normal growth, the C-terminal domain of Tfb3 (which is part of the Kinase Module) is not
166 essential for viability.

167 **Expression of the TFIIH Core and Kinase Modules as independent complexes.** Recent
168 structural studies show that the C-terminal domain of Tfb3, or its metazoan homolog MAT1,
169 stabilizes an active kinase conformation when bound to Kin28/CDK7 and its partner cyclin (19-

170 21). Therefore, the slow growth of strains lacking the Tfb3 C-terminal domain could be due to
171 loss of kinase tethering to the Core Module, to loss of Kin28/CDK7 activation, or both.
172 To test the contribution of the Tfb3 kinase activation function separately from kinase
173 tethering, parts of Tfb3 were expressed as two separate proteins (**Fig. 2C**). Strains expressing
174 either the N-term (left panel) or N-term-Linker (right panel) derivatives were transformed with
175 plasmids expressing the indicated C-terminal (C-term) domain constructs. These strains were
176 tested for growth by serial dilution spotting, where the size of single colonies serves as a
177 measure of relative growth rate. Again, strains lacking any C-term domain grew very slowly
178 (Vector, top row). In the N-term strain (left panel), adding wild-type Tfb3 restored growth to
179 normal. Co-expression of the separate N-term and C-term domains noticeably improved growth
180 compared to N-term alone, despite the fact that this strain completely lacks the Linker region.
181 Co-expression of the Linker-C-term construct rescued growth to an even greater extent,
182 although not quite to wild-type rates. Therefore, the Linker does contribute to full function of
183 the Kinase Module.
184 Unexpectedly, expression of the N-term-Linker construct (**Fig. 2C**, right panel) had a
185 dominant negative effect, as it caused slow growth even in the presence of WT Tfb3 (right
186 panel, second row). Nonetheless, some growth improvement was seen by co-expressing C-
187 term, but only using a high copy plasmid likely to produce more protein. Co-expressing the
188 Linker-C-term construct gave a similar growth improvement, but at both high and low copy.
189 Altogether, the co-expression results show that the Tfb3 N-terminal and C-terminal domains
190 can function independently of covalent physical linkage, and suggest that the Linker region
191 primarily contributes to function of the Kinase Module.
192 We considered the possibility that, despite the split Tfb3, the TFIIH Kinase and Core
193 Modules could remain associated through other subunit contacts. To test this possibility, a
194 tandem affinity purification (TAP) tag was used to precipitate full-length, C-term, or Linker-C-
195 term Tfb3 derivatives using IgG beads. While there was some variation in protein levels (**Fig.
196 3A**, left panel, lanes 1-4), similar amounts of all three TAP fusions were precipitated with IgG
197 beads (lanes 5-8). The Kinase Module was intact, as subunits Kin28 and Ccl1 interacted with
198 full-length or Tfb3 C-terminal constructs equally well (**Fig. 3B**). An in vitro phosphorylation assay
199 using GST-CTD as substrate showed that Kinase Modules from the truncated Tfb3 alleles
200 retained activities similar to or slightly below that of full-length Tfb3 (**Supplemental Fig. S2**).
201 In contrast to the Kinase Module, the TFIIH Core Module (monitored by Core subunit
202 Tfb1) no longer associates strongly with the uncoupled Tfb3 C-term derivatives (**Fig. 4A**,
203 compare lanes 3 and 4 to full-length Tfb3 in lane 2). The Linker-C-term derivative may retain
204 some weak interaction with the Core, but the Tfb1 levels were just slightly above background
205 binding in the untagged strain (lane 1), and far below that seen with full length Tfb3. We
206 conclude that the split Tfb3 does indeed dissociate the two TFIIH modules.
207 The basal transcription factor TFIIE directly contacts several Core TFIIH subunits,
208 including Tfb3, within the RNApII PIC. Furthermore, TFIIE stimulates TFIIH enzymatic activities,
209 including the kinase (30). To test how the TFIIE-TFIIH association was affected by the split Tfb3,
210 the TAP-precipitated samples were also immunoblotted for the TFIIE subunits Tfa1 and Tfa2.
211 Whereas full length Tfb3 efficiently pulls down both TFIIE subunits, the separated C-term or
212 Linker-C-term derivatives do not **(Fig. 4B)**. This result further indicates that the Kinase Module

213 no longer associates with the TFIIH Core or the RNApII initiation complex upon splitting Tfb3
214 into two parts.
215 **Uncoupling the TFIIH modules disrupts proper kinase localization.** Given the viability
216 of the split Tfb3 strains, we wondered if the untethered Kinase Module was still delivered to
217 promoters, perhaps via interaction with Mediator. Genome-wide chromatin
218 immunoprecipitation (ChIP-Seq) was used to compare localization of the TFIIH modules in the
219 wild-type and split Tfb3 strains. In cells expressing full-length Tfb3, the Core TFIIH subunit Tfb1
220 showed a strong peak near the transcription start site, reflecting promoter localization in the
221 PIC (**Fig 5A and Supplemental Fig. S3A**, red line**)**. In all three split Tfb3 strains (yellow, blue, and
222 green), the Tfb1 signal was reduced relative to the full-length, but still clearly promoter-
223 localized. Perhaps reflecting reduced PIC formation, a similar reduction was seen for RNApII
224 subunit Rpb1 (**Fig 5D and Supplemental Fig. S3D**). Interestingly, the Tfb1 signal was closest to
225 normal in the strain in which the Linker was fused to the N-terminal domain, despite the fact
226 that this strain grew slower than strains with the Linker on the C-terminal domain or missing
227 completely (**Fig 2C**). In contrast to Core TFIIH, the Kin28 ChIP signal, normally localized at
228 promoters in wild-type Tfb3 strains, was completely absent in all the split Tfb3 strains (**Fig 5B**
229 and **Supplemental Fig. S3B**). Therefore, although Core TFIIH is still properly localized, the
230 untethered Kinase Module is no longer recruited to promoters.
231 **Untethered kinase module leads to aberrant Ser5P patterns.** We expected that loss of
232 Kinase Module recruitment would affect CTD Serine 5 phosphorylation (Ser5P) negatively, with
233 possible indirect effects on Ser2P and overall elongation processivity. This prediction was first
234 tested using immunoblotting of whole cell extracts. Cells lacking any Tfb3 C-term were strongly
235 reduced for both Ser5P and Ser2P (**Supplemental Fig. S4**, lanes 2 and 3). Similar to the growth
236 phenotypes, adding back the C-term as a separate protein greatly improved CTD
237 phosphorylation levels at both sites, albeit not to full wild-type levels (lanes 4 and 5).
238 ChIP-seq was used to determine the location of Ser5P, normalizing to spiked-in *S. pombe*
239 chromatin. Surprisingly, the restored Ser5P was abnormally distributed in split Tfb3 cells. Total
240 RNApII crosslinking (**Fig 5D and Supplemental Figs. S3D and S5A, B**) was reduced in the
241 mutants, but the levels remained consistent across the gene. This pattern argues against an
242 elongation processivity defect in the split Tfb3 strains, and contrasts with the 5' to 3' drop seen
243 upon complete depletion of Kin28 (31) or Bur2, the cyclin for the elongation kinase Bur1/Cdk9
244 (32). Ser5P normally has a strong peak at promoters, and lower but significant levels
245 throughout transcribed regions, as can be seen in both individual gene traces (**Supplemental**
246 **Fig. S4A, B**, promoters in green boxes) and metagene analysis (**Fig 5C** and **Supplemental Fig.**
247 **S3C**, red curves). In the split Tfb3 strains, the Ser5P promoter peak was missing, but levels of
248 this modification remained high throughout the downstream transcribed region.
249 Normalization of Ser5P to total RNApII indicated that downstream Ser5P was actually elevated
250 in the mutants relative to wild-type (**Fig 5E**).
251 Quantitation of RNApII-normalized Ser5P at individual genes (**Supplemental Fig. S3E, F**)
252 showed that this redistribution of Ser5P occurred at virtually all genes. The Ser5P signals at
253 promoters are reduced by up to 50%, particularly at strongly transcribed genes (i.e. those with
254 highest Rpb1 signal), with the distribution for the mutant/WT ratio is centered around one for
255 the weakest genes (**Supplemental Fig. S3E**, left panels). In contrast, the normalized Ser5P
256 signal in open reading frames (right panels) are nearly all increased by two-fold or more in the

257 mutants. Despite the changes in CTD phosphorylation, the steady RNApII levels across genes in
258 the mutants (**Fig 5D**) suggests no defect in elongation processivity. Using the total Rpb1 signals
259 as a measure of transcription levels, it can be seen that transcription is clearly down overall in
260 the split Tfb3 strains (**Supplemental Fig. S3F**). The exceptions were seven genes with
261 reproducibly increased Rpb1 signals. All but one of these were known heat shock response
262 genes (**Supplemental Fig. S3G**), suggesting these slow growing cells are under stress.
263 ChIP-seq was also performed for Ser2P. While the overall signals were too low to get
264 good quality data for metagene analysis, individual gene traces at strongly transcribed genes
265 suggested that the pattern of Ser2P was relatively normal (**Supplemental Fig. S5B**). In both WT
266 and split Tfb3 strains, Ser2P was lowest near the promoter and gradually increased further
267 downstream.
268 The surprising increase of Ser5P downstream of the promoter suggests that the Tfb3
269 linkage not only delivers the Kinase Module to the promoter, but may also inhibit its activity
270 outside of the PIC. Transcription-associated phosphatases normally cause Ser5P to drop soon
271 after RNApII enters the body of the gene (reviewed in (14, 26, 27)), so the higher downstream
272 Ser5P signal suggests untethered kinase module may be able to continually access the CTD
273 during elongation. This could be due to inhibition of TFIIH Core-associated Kinase outside of
274 the PIC, or suggest that the majority of TFIIH is sequestered at promoters and therefore
275 unavailable at later stages of transcription.
276 **Disconnected Core TFIIH does not cause an NER defect.** The TFIIH Core Module also
277 functions as a key component of the NER machinery, and Tfb3 has been shown to be important
278 for this function (29). While many mutations in Core subunits therefore cause sensitivity to
279 ultraviolet (UV) light, this is not the case for Kinase Module mutants. Recent structures
280 (reviewed in (11)) show that the Kinase Module would block interactions between the Core
281 Module and other NER factors. Therefore, TFIIH either enters into the NER complex as free Core
282 Module, or the Kinase Module must dissociate soon after. We tested the response to UV light in
283 strains where the split Tfb3 dissociates the Core and Kinase Modules (**Fig. 6**). Two wild-type
284 Tfb3 strains acted as controls for normal UV response, including one strain lacking the Tfb6
285 protein that competes with the Core for Ssl2 binding (33), as this background was used for
286 many experiments here (see **Supplemental Table S2**). None of the split Tfb3 configurations
287 caused UV sensitivity, indicating that the separated N-term of Tfb3 is sufficient for the Core NER
288 function. In fact, we noticed that strains with free N-term domain, where the linker is either
289 absent or connected to the C-terminal domain, may even have slight resistance to UV light,
290 consistent with a model in which the Kinase Module inhibits the TFIIH NER function.
291

292 **DISCUSSION**

293 We show here that the TFIIH Core and Kinase Modules can be uncoupled in vivo (**Fig. 2**).
294 Although it was previously reported that both the N-term and C-term of Tfb3 are essential for
295 viability in *S. cerevisiae* (22, 29), we found that cells lacking the C-terminal domain are viable
296 but extremely slow growing. Indeed, accurate transcription initiation can be reconstituted in
297 vitro using a Tfb3 truncation consisting of only N-term residues 1-148 (34). While fusion of
298 other kinase modules to the Tfb3 linker did not substitute for the C-term (**Fig. 1**), we found that
299 adding back the Tfb3 C-terminal domain as a separate protein dramatically improved growth
300 (**Fig. 2**). This rescue results from the restored CTD kinase activity of the untethered Tfb3 C-
301 term/Kin28/Ccl1 complex (**Figs. 3, S2, and S4**). Notably, Mouse Embryonic Fibroblasts and
302 cardiomyocytes with a homozygous deletion of *MAT1* were shown to be viable but abnormal
303 (35, 36). In these cells, Core TFIIH remains intact, but levels of the Kinase Module proteins CDK7
304 and Cyclin H are severely reduced. *MAT1* deletion leads to major defects in CTD
305 phosphorylation and transcription, but the effects are partially compensated by reduced mRNA
306 degradation rates. Therefore, our yeast results splitting the Core and Kinase Modules are likely
307 also applicable to mammalian TFIIH.

308 *Separating the Core and Kinase Modules leads to misregulated CTD phosphorylation.*
309 ChIP-Seq showed that Kin28 kinase was no longer recruited to promoters in the split Tfb3
310 strains, even though Core TFIIH still showed proper localization (**Figs. 5 and S3**). Having
311 uncoupled the Kinase Module from TFIIH, we expected CTD Ser5P to be severely reduced in the
312 split Tfb3 strains. Indeed, Ser5P peaks at promoters were largely gone, but instead the
313 modification was found throughout the downstream transcribed region at levels higher than
314 normal **Figs. 5, S3, and S5**). This pattern suggests the untethered Kinase Module can access the
315 CTD during elongation in a way that the intact TFIIH cannot. A surprising implication is that, in
316 addition to delivering the kinase to the initiation complex, the connected TFIIH Core may help
317 limit CTD phosphorylation to early transcription. We previously showed that CTD kinase activity
318 of free trimer Kinase Module was less sensitive than TFIIH complex to mutations in the
319 activating T-loop (37). Therefore, the Core module may have some inhibitory effect on CTD
320 kinase activity that is relieved when TFIIH is incorporated into the PIC. However, precipitates
321 with full-length Tfb3 did not have less kinase activity than those from split Tfb3 cells
322 (**Supplemental Fig. S2**). An alternative possibility is that, under normal conditions, the majority
323 of Kinase Module is tethered to the Core at promoters and therefore sequestered from
324 phosphorylating downstream RNApII.

325 Increased downstream Ser5 phosphorylation in the split Tfb3 strain raises an interesting
326 question about normal CTD phosphorylation patterns. The earliest ChIP experiments (38), as
327 well as subsequent ChIP-seq studies, detected some Ser5P throughout transcribed regions.
328 Mass spectrometry of RNApII associated with the mRNA termination factor Rtt103 also
329 detected significant Ser5P in late elongation (39). It has been presumed that this downstream
330 signal represented residual phosphatase-resistant Ser5P acquired at the promoter. However, an
331 alternative model that must now be considered is that free Kin28/Cdk7 kinase trimer continues
332 to carry out de novo phosphorylation throughout the transcription cycle, transiently interacting
333 with elongating RNApII. Free CDK7/Cyclin H/MAT1 trimer exists in metazoans to provide CAK
334 activity, but free yeast Kin28/Ccl1/Tfb3 trimer is also detected in yeast (37). A dynamic
335 equilibrium between kinase and phosphatase activities regulate CTD Serine 2 phosphorylation

336 during elongation (24), and a similar dynamic may exist for Ser5P well downstream of
337 promoters.
338 *Communication between the Core and Kinase Modules.* The viability of a split Tfb3 strain
339 completely lacking the linker might suggest this central region serves only to tether the N- and
340 C-terminal domains. However, available TFIIH structures and our data suggest otherwise. Cells
341 expressing a Linker-C-term fusion grew better than cells completely lacking the linker. In
342 contrast, The N-term-Linker fusion protein acts as a dominant negative allele, slowing growth
343 even in the presence of wild-type Tfb3 (**Fig. 2C**). These results suggest linker has a function
344 beyond simply tethering the two modules. To address this question, it is informative to
345 compare the available structures for free TFIIH complex, TFIIH incorporated into the PIC, and
346 TFIIH as part of the NER machinery (reviewed in (11)). The Core Module has a horseshoe shape,
347 with the TFIIH ATPases, Ssl2/XPB and Rad3/XPD, at the two ends (see **Fig. 7** schematic). The
348 spacing between the ATPases changes substantially depending on context. In free TFIIH, the
349 long alpha-helix in the Tfb3/MAT1 Linker spans from Tfb3 N-term, which is contacting
350 Rad3/XPD, to the other side of the horseshoe, where it directly contacts Ssl2/XPB (**Fig. 7A**).
351 Here, the central Linker domain serves to lock together the two TFIIH ATPases in a "closed"
352 conformation. In the PIC, the Tfb3/MAT1 alpha-helix is disconnected from Ssl2/XPB, producing
353 an "open" conformation with the Ssl2/XPB rotated outward, its active site bound to the double-
354 stranded DNA downstream of RNApII (**Fig. 7B**). TFIIH within the NER complex lacks the Kinase
355 Module, and in this case the NER factors bring Rad3/XPD and Ssl2/XPB even closer together to
356 facilitate the interaction of the damaged DNA with both ATPase active sites (11).
357 A recent report describing two new PIC structures (40) shows that when the +1
358 nucleosome blocks Ssl2/XPB from downstream DNA, TFIIH is in the closed conformation, with
359 the Tfb3/MAT1 Linker contacting both ATPases. Positioning the nucleosome further
360 downstream allows the open TFIIH conformation, resulting in loss of the contact between the
361 Tfb3/MAT1 Linker and Ssl2/XPB. Notably, much of the Tfb3 long alpha-helix becomes
362 disordered when disconnected from Ssl2/XPB. Although these two new PIC structures lack
363 Mediator, and it hasn't been shown that the closed TFIIH PIC is actually a necessary precursor
364 to the open TFIIH, it seems quite plausible that TFIIH enters the PIC in the closed conformation,
365 but transitions to the open conformation upon DNA binding in order to proceed with DNA
366 translocation and promoter melting.
367 Based on our findings, we speculate that the Tfb3 Linker could provide a mechanism for
368 temporal coupling of TFIIH kinase and promoter melting functions (**Fig. 7B**). PICs with closed
369 TFIIH are predicted to be inhibited for ATP hydrolysis by Ssl2/XPB (40), and as described above,
370 may also be partially inhibited for kinase activity. We propose that movement of the Kinase
371 Module in the PIC repositions the Tfb3 Linker to release the inhibitory contact with Ssl2/XPB,
372 freeing the translocase for promoter melting. This movement may involve capture of the
373 Kinase Module by Mediator, and perhaps even CTD phosphorylation. Supporting the idea that
374 the Kinase Module is mobile, PICs formed in vitro without Mediator show the Kinase Module
375 close to the Rpb4/Rpb7 stalk of RNApII (40, 41), far from its position seen when interacting with
376 Mediator. CTD phosphorylation triggers release of Mediator (42), and in vivo experiments with
377 TFIIH kinase inhibition suggests this transition occurs very rapidly after PIC formation (31, 43).
378 Notably, release of the Tfb3 Linker contact also results in the long alpha-helix becoming
379 disordered (40), which could allow the kinase access to a far larger radius of area. This flexibility

380 could help the kinase reach both proximal and distal repeats within the CTD, which can
381 theoretically extend quite far from the RNApII body.
382 It has long been known that yeast PICs access transcription start sites (TSSs) far further
383 downstream than metazoan PICs. Enzymatic studies show that for yeast TFIIH, but not its
384 mammalian homolog, the Kinase Module greatly stimulates the processivity of the Ssl2
385 translocase activity necessary for downstream TSS scanning (44). This effect is dependent on
386 the presence of the Kinase Module, but not kinase activity. Interestingly, yeast transcription
387 reconstituted in vitro with TFIIH lacking Tfb3 and the Kinase Module causes a dramatic
388 upstream shift in transcription start sites, with the TATA-TSS spacing now resembling that of
389 metazoans (45). This effect can be reversed by adding back only the Tfb3 N-term (34), arguing
390 against a model where the contact between Tfb3 linker and Ssl2 is necessary for downstream
391 TSS usage. Nevertheless, there is clearly some communication between the Kinase and Core
392 Modules, and Tfb3 is likely to be a key link.
393 *Evolutionary considerations.* We speculate that cells with a complete deletion of the
394 Tfb3 Linker could resemble an evolutionarily ancient state where TFIIH Kinase and Core existed
395 as completely distinct enzymes. Initially, the primary role of TFIIH Core was almost certainly
396 NER, and the Kinase Module precursor probably functioned to phosphorylate CDKs or other
397 substrates. It is likely each was independently co-opted for RNApII transcription. Supporting this
398 hypothesis, TFIIH in the early diverged eukaryote *Trypanosome brucei* appears to consist of only
399 the Core Module, as no Tfb3 or other Kinase Module homologs are found in the purified
400 enzyme complex or by sequence similarity search (46, 47). The *T. brucei* CTD is quite diverged,
401 without the typical repeat sequence found in most eukaryotes (48, 49). In the main eukaryotic
402 lineage, the Tfb3 Linker likely evolved over time to coordinate the timing of CTD
403 phosphorylation and promoter melting.
404 In the split Tfb3 strains, fusion of Linker to the C-term domain may improve growth
405 relative to the complete Linker deletion by partially restoring kinase-translocase coupling. In
406 contrast, the observed toxicity of the Tfb3 N-term-Linker fusion may result from the Core TFIIH
407 being locked into the closed conformation. Our ChIP-Seq results suggest an ancestral, free CTD
408 kinase may have acted throughout elongation. Tethering the kinase to TFIIH would have
409 targeted high levels of CTD phosphorylation during early transcription, and may also have
410 opened the door for the CTD Code as we know it today, where distinct phosphorylation
411 patterns to mark the progression of the transcription cycle.
412
413

414 **Acknowledgements**
415 We are grateful to Steve Hahn (FHCRC, Seattle) and John Feaver (Stanford) for providing
416 several Tfb3 strains and plasmids, and to Jason Tanny (McGill Univ., Montreal) for *S. pombe*
417 cells. This work was supported by a grant from the Canadian Institutes of Health Research
418 (CIHR; PJT-162334) to F.R., and by US NIH grants GM046498 and GM056663 to S.B.
419
420 **METHODS**
421
422 **Plasmid construction and Yeast Strains**. Plasmids used in this study, and their
423 construction, are listed in **Supplemental Table S1**. Yeast strains used in this study are listed in
424 **Supplemental Table S2**.
425 **Antibodies and Immunoblotting.** The following primary antisera were used: anti-Ccl1
426 (37), anti-Kin28 (Covance, PRB-250C-500), anti-Tfb1 (50), anti-Tfa1 and anti-Tfa2 (51), anti-
427 Ser2P (3E10), anti-Ser5P (3E8) (gift from Dirk Eick (52)), anti-CTD (8WG16) , anti-Rpb3
428 monoclonal 1Y26 (BioLegend). For immunoblotting, primary antibodies were used at a 1:1000
429 dilution. Secondary antibodies coupled to horse radish peroxidase (goat anti-rabbit, goat anti-
430 rat, and goat anti-mouse) were purchased from Sigma and used at the recommended dilution.
431 Anti-Tfb3 antibodies (37) were affinity purified from sera to reduce cross-reacting
432 signals. Briefly, recombinant Tfb3 protein was expressed from plasmid pSBEThis7-Tfb3 in *E. coli*
433 BL21(DE3). Cells were grown at 37°C to an OD_{600} of 0.4-0.6 in 4 L of selective media. Expression
434 was induced with 0.2mM IPTG and cultures were incubated shaking at 30°C for 4 hrs. Cells were
435 pelleted and resuspended in 100 mL lysis buffer (1X PBS, 1% SDS, pH 7.4). After sonication, cell
436 debris was pelleted at 23,970 g for 20 min. The supernatant was filtered and then incubated
437 with nutation at 4°C for 1 hr with Ni-NTA agarose (Gold Biotechnology #H-350-100) that was
438 pre-equilibrated with lysis buffer. Lysate and beads were drained through a column and washed
439 extensively with wash buffer (1X Phosphate Buffered Saline (PBS), 0.1% Sarkosyl, 10 mM
440 imidazole, pH 7.4). Bound protein was serially eluted with elution buffer (1X PBS, 0.1% Sarkosyl,
441 pH 7.4) supplemented with increasing imidazole concentrations (1 mL each): 50 mM, 100 mM,
442 150 mM (2X), 200 mM, 300 mM. Fractions with the highest Tfb3 yield were pooled. Roughly 2
443 mg of purified Tfb3 was covalently linked to 1 ml AminoLink® Plus Coupling Resin (Thermo
444 Scientific #PI20505) following the manufacturer's protocol for crosslinking at pH 10 with
445 cyanoborohydride solution. Specific anti-Tfb3 antibodies were affinity purified from crude
446 antiserum as described (53). Tfb3-coupled beads were serially washed with 10 bed volumes
447 each of 10 mM Tris pH 7.5, 100 mM glycine pH 2.5, 10 mM Tris pH 8.8, and then 100 mM
448 triethylamine pH 11.5. Finally, beads were poured into a small column and washed with 10 mM
449 Tris pH 7.5 until pH reached 7.5. Antiserum was diluted 1:10 with 10 mM Tris pH 7.5 and passed
450 through the column three times. The column was then washed with 20 bed volumes each of 10
451 mM Tris pH 7.5 and 500 mM NaCl, and then 10 mM Tris pH 7.5. Bound antibodies were serially
452 eluted with small volumes of high (100 mM triethylamine pH 11.5) and low (100 mM glycine pH
453 2.5) pH, followed by rapid neutralization. Peak fractions were pooled and concentrated using
454 Amicon Ultra 0.5 10K Concentrator, with PBS as the replacement buffer.
455 **Yeast whole cell extracts.** Two types of extracts were used for gel electrophoresis and
456 immunoblotting, with similar results. The first is an alkaline lysis method. 1.5 mL of late log
457 phase liquid culture was pelleted at 4,600 g for 90 sec at room temperature. Media was

458 removed, and the pellet was resuspended in 0.1 M NaOH and incubated at room temperature
459 for 5 min. Cells were pelleted at 9,300 g for 90 sec at room temperature, supernatant was
460 removed, and pellet was resuspended in 60 µL lysis buffer (0.06 M Tris-HCl pH 6.8, 5% glycerol,
461 2% SDS, 4% β-mercaptoethanol, 0.0025% bromophenol blue) (54). Samples were heated at
462 95°C for 5 min, pelleted at 9,300 g for 1:30 min at room temperature, and supernatant was
463 collected to run on an SDS-PAGE gel.
464 For some gels, a non-denaturing whole cell extract was used. First, 1.0-1.5 mL of liquid
465 culture was pelleted (all centrifugations were at 2,300 g) at 4°C for 2 min and washed with 1 mL
466 cold distilled water. Pellets were resuspended in 100 µL cold lysis buffer (50 mM HEPES pH 7.6,
467 1 mM EDTA, 300 mM NaCl, 20% glycerol, 1 mM DTT, 1 µg/mL leupeptin, 1 µg/mL aprotinin,
468 1 µg/mL pepstatin A, and 1 µg/mL antipain). The resuspension was mixed with 100 µL 425-600
469 µm glass beads (Sigma, #G8772-1KG) and vortexed at 4°C for 10 min. Extract was centrifuged
470 for 10 min at 4°C and supernatant collected. Total protein concentration of extracts was
471 measured using NanoDrop 2000 Spectrophotometer (ThermoScientific)**.**
472 **TAP purification and co-precipitation assay**. TAP-tagged Tfb3 derivatives were used for
473 assaying Kinase Module association and in vitro kinase assays. Yeast strains were grown in 200
474 mL of selective media at 30°C to an OD_{600} of ~2. Cells were collected by centrifugation, flash
475 frozen in liquid nitrogen, and lysed using a SPEX SamplePrep Freezer Mill 6875D with small
476 chambers. Pulverized cells were resuspended by rotation at 4°C in 1 mL of lysis buffer (20 mM
477 HEPES pH 7.6, 10% glycerol, 200 mM KoAc, 1 mM EDTA, 1 mM DTT, 1 mM NaF, 1 mM Na3VO4,
478 1 µg/mL leupeptin, 1 µg/mL aprotinin, 1 µg/mL pepstatin A, 1 µg/mL antipain, 1 mM PMSF)
479 until homogeneous. Cell debris was pelleted in a benchtop microfuge at 4,500 g for 25 min, and
480 supernatant was collected and further cleared in a microfuge at maximum speed for 10 min. All
481 centrifugations were done at 4°C. The clear layer of lysate was transferred to a new tube, 10 µL
482 of IgG Sepharose (GE Healthcare, #17096901) pre-equilibrated with lysis buffer was added, and
483 the suspension was rotated at 4°C for 1 hr. After binding, IgG beads were gently pelleted,
484 supernatant was removed, and beads were washed 3 times with lysis buffer.
485 For analysis of bound proteins, 50 µL of 2X SDS-PAGE sample buffer (0.1% bromophenol
486 blue, 0.2 M DTT, 20% glycerol, 4% SDS, 0.1 M Tris-Cl pH 6.8) were added to the beads and the
487 sample was heated at 100°C for 5 min. The beads were then pelleted by centrifugation,
488 supernatant was collected, and samples were analyzed by immunoblotting. Input, flowthrough,
489 and final samples from the co-immunoprecipitation protocol were run on 10% polyacrylamide
490 SDS-PAGE gels. Proteins were transferred to polyvinylidene difluoride (PVDF) membranes.
491 Membranes were blocked with 5% powdered milk in Tris Buffered Saline with 0.1% Tween and
492 then probed with the appropriate primary antibody. Blocking and antibody incubations were
493 done for either 1 hr at room temperature or overnight at 4°C. Following several washes, the
494 blots were incubated with secondary antibody at a 1:10,000 dilution for 1 hr. Reacting bands
495 were detected by chemiluminescent detection using the Thermo SuperSignal Plus Pico kit
496 according to the manufacturer's instructions.
497 **In vitro CTD phosphorylation assay.** IgG beads were used to immobilize the Tfb3-TAP
498 derivatives as described above. After normalizing for the amount of Kin28, beads were
499 incubated with 100 ng GST-CTD in 1x kinase reaction buffer (20 mM HEPES pH 7.6, 7.5 mM
500 MgOAc, 2% Glycerol, 100 mM KOAc, 2 mM DTT, and 25 µM ATP). Samples were taken at 15, 30,

501 and 60 min, and phosphorylation was assayed by immunoblotting with anti-Ser5P (3E8)
502 antibody.
503 **ChIP-seq.** ChIP experiments were performed from two independent biological replicates
504 as previously described (55). Yeast cultures were grown in 50 mL of selective medium at 30°C to
505 an OD_{600} of 0.7-0.9 before crosslinking with 1% formaldehyde (Fisher Scientific, BP531-500) at
506 room temperature for 30 min and quenched with 125 mM glycine. Crosslinked cells were
507 collected by centrifugation and washed twice with 1X TBS (20 mM Tris-HCl pH 7.5, 150 mM
508 NaCl). Cell pellets were then resuspended in 700 µL Lysis buffer (50 mM HEPES-KOH pH 7.5, 140
509 mM NaCl, 1 mM EDTA, 1% Triton X-100, 0.1% Na-deoxycholate and protease inhibitor cocktail
510 (1 mM PMSF, 1 mM benzamidine, 10 µg/mL aprotinin, 1 µg/mL leupeptin, 1 µg/mL pepstatin
511 A)). About the same number of OD_{600} units was used for all samples. A fixed amount of
512 crosslinked *Schizosaccharomyces pombe* cells (a gift from Jason Tanny), at 10% the amount of *S.*
513 *cerevisiae* cells, was added for normalization as previously described (56). Cells were lysed by
514 bead beating and the lysate was sonicated with a Model 100 Sonic dismembrator equipped
515 with a microprobe (Fisher Scientific), 4 x 20 sec at output 7 Watts, with a 1 min break between
516 sonication cycles. Soluble fragmented chromatin was recovered by centrifugation. 600 µL of the
517 chromatin sample was taken per immunoprecipitation (IP) and 6 µL (1%) was saved as an Input
518 sample. The following amounts of antibody per IP were used: anti-RNApII Rpb1 8WG16 (2 µg),
519 anti-Ser5P 3E8 (5 µL), anti-Tfb1 (4 µL) and anti-Kin28 (4 µL). All antibodies have been validated
520 for ChIP. Anti-Ser5P 3E8, anti-Tfb1, and anti-Kin28 antibodies were coupled to Dynabeads
521 coated with Protein G (Thermo Fisher Scientific, 10004D) and anti-RNApII Rpb1 8WG16
522 antibody was coupled to Dynabeads coated with Pan Mouse IgG antibodies (Thermo Fisher
523 Scientific, 11042). 50 µL of the appropriate Dynabeads pre-coupled with the indicated antibody
524 were added to the chromatin sample and incubated overnight at 4°C. Beads were washed twice
525 with Lysis buffer, twice with Lysis buffer 500 (Lysis buffer + 360 mM NaCl), twice with Wash
526 buffer (10 mM Tris-HCl pH 8.0, 250 mM LiCl, 0.5% NP40, 0.5% Na-deoxycholate, 1 mM EDTA)
527 and once with TE (10 mM Tris-HCl pH 8.0, 1 mM EDTA). Input and immunoprecipitated
528 chromatin were eluted and reverse-crosslinked with 50 µL TE/SDS (TE + 1% SDS) by incubating
529 overnight at 65°C. Samples were treated with RNase A (345 µL TE, 3 µL 10 mg/mL RNAse A
530 (Sigma-Aldrich, R6513), 2 µL 20 mg/mL Glycogen (Roche, 10901393001)) at 37°C for 2 hr and
531 subsequently subjected to Proteinase K (15 µL 10% SDS, 7.5 µL 20 mg/mL Proteinase K (Thermo
532 Fisher Scientific, 25530049)) digestion at 37°C for 2 hr. Samples were extracted twice with
533 phenol/chloroform/isoamyl alcohol (25:24:1), followed by precipitation with 200 mM NaCl and
534 70% ethanol. Precipitated DNA was resuspended in 50 µL of TE before being used in ChIP-seq
535 libraries.
536 All ChIP and Input samples were subjected to a 1.7X cleanup using KAPA Pure Beads
537 (Roche, 07983280001) according to the manufacturer's instructions. Samples were eluted with
538 40 µL of Elution buffer (10 mM Tris pH 8.0). DNA concentration of ChIP and Input samples was
539 determined by qPCR using a standard curve made with a fragment size control sample. 1-10 ng
540 of ChIP and Input DNA were used for ChIP-seq library preparation as follows. The ends of DNA
541 were repaired by incubating in 70 µL of 1X NEBuffer 2 containing 0.6 units of T4 DNA
542 polymerase (NEB, M0203S), 2 units of T4 polynucleotide kinase (NEB, M0201S), 0.09 nM dNTPs
543 and 0.045 µg/µL of BSA at 12°C for 30 min. Repaired DNA was then subjected to a 1.7X cleanup
544 using KAPA Pure Beads before dA tailing as follows. Beads containing the repaired DNA were

545 resuspended in 50 µL of 1X NEBuffer 2 containing 0.1 mM dATP and 25 units of Klenow
546 Fragment (3'→5' exo-) (NEB, M0212M), and incubated at 37°C for 30 min. After a 1.8X cleanup
547 with KAPA Pure Beads, the A-tailed DNA was ligated to index adapters (Illumina Truseq DNA UD
548 Indexes (20023784)) as follows. The beads were resuspended in 45 µL of 1X Ligase buffer
549 containing 8 nM of adapter and 2.5 units of T4 DNA ligase (ThermoFisher, 15224041) and
550 incubated at room temperature for 60 min. The ligated DNA was then subjected to a 1X
551 cleanup with KAPA Pure Beads, followed by a double size selection (0.52X-1X) leading to
552 fragments in the 200-600 bp range. Libraries were PCR-amplified with 12-13 cycles using KOD
553 Hot Start DNA polymerase (Millipore, 71086-3) and cleaned up using 1X KAPA Pure Beads.
554 Libraries were qualified on Agilent 2100 Bioanalyzer using High Sensitivity DNA Kit and
555 quantified by qPCR using NEBNext Library Quant Kit for Illumina (NEB, E7630). Equal molarity of
556 each library was pooled and subjected to sequencing on Illumina NovaSeq 6000 platform at the
557 McGill University and Génome Québec Innovation Centre to generate 100 bp paired-end reads.
558 **ChIP-seq Data analysis**. ChIP-seq data was analyzed as previously described (55).
559 Adapter sequences were removed from paired-end reads for each biological replicate using
560 Trimmomatic, version 0.36 (57) with parameters "ILLUMINACLIP:adapters.fa:2:30:10:
561 TRAILING:3 MINLEN:25". Paired-end reads for each biological replicate were independently
562 aligned to the *S. cerevisiae* (UCSC sacCer3) and *S. pombe* (Downloaded from
563 https://www.pombase.org/ on December 7th 2022) reference genomes using the short read
564 aligner Bowtie 2 (version 2.3.4.3) (58). Only reads mapped in proper pairs and primary
565 alignments were kept in aligned files using Samtools, version 1.9 (59) with parameters "-F 2048
566 -F 256 -f 2". Duplicate reads were removed from aligned files using Samtools "fixmate" and
567 "markdup -r". Coverage for each base pair of the *S. cerevisiae* genome was computed using
568 genomeCoverageBed from BEDTools, version 2.27.1 (60) and normalized using *S. pombe* reads
569 as follows. The read density at each position of the *S. cerevisiae* genome was multiplied by a
570 normalization factor N defined as:
571
572 $N = 1{,}000{,}000 * P / R * C$
573 where:
574 1,000,000 is an arbitrarily chosen number used for convenience;
575 *R* is the total number of reads in the IP sample that mapped to the *S. pombe* genome;
576 *C* is the total number of reads in the Input sample that mapped to the *S. cerevisiae*
577 genome;
578 *P* is the total number of reads in the Input sample that mapped to the *S. pombe* genome.
579
580 The deduplicated BAM files of replicates were merged using Samtools "merge".
581 Correlation between replicates were generated using deepTools, version 3.5.1 (61) with
582 parameters "multiBigwigSummary bins --binSize 100" and "plotCorrelation --corMethod
583 pearson --whatToPlot heatmap --colorMap PiYG --plotNumbers".
584 The genome coverage files were converted to the bigWig format using the utilities from
585 UCSC Genome Browser (62).
586 Statistics regarding the reads (including the number of reads, mapped reads, the
587 correlation between replicates, etc.) are shown in **Supplemental Table S3**.

588 The RNApII-adjusted Ser5P coverage file (used in **Fig. 5E** and **Supplemental Fig. S3E**) was
589 generated as follows, starting from *S. pombe*-normalized coverage files. For each genomic
590 position, the Ser5P occupancy value of a given Tfb3 mutant was multiplied by the RNApII
591 occupancy value in WT and divided by the RNApII occupancy value in the mutant.
592 Aggregate profiles (metagene analyses) were generated using the Versatile Aggregate
593 Profiler (VAP) (63, 64). The aggregate profiles were generated by aligning data on the
594 transcription start site (TSS) and the polyadenylation (pA) signal of all verified genes that have a
595 signal of RNApII >4 and are longer than 1 kb (n=95). The data were averaged over 10 bp bins.
596 TSS and pA site coordinates were from Pelechano et al. (65).
597 In **Supplemental Fig. S3E**, the values for "promoters" are the average signal over a 200
598 bp window centered on the TSS whereas the values for "ORFs" are the average of the signal
599 between position +200 and the pA site. The region between +100 and +200 was excluded to
600 avoid signal contamination from promoters for ORFs and vice versa.
601 All raw and processed ChIP-seq data generated in this study have been deposited in the
602 NCBI Gene Expression Omnibus (GEO; http://www.ncbi.nlm.nih.gov/geo/) under accession
603 number GSE241436.
604 **UV sensitivity assay:** Yeast strains were grown in liquid media selective for the *TFB3*
605 plasmids, and overnight cultures were diluted to an OD_{600} = 0.005 and 0.0005 for plating. For
606 each test plate, 100 μL of diluted cells were spread on selective media. Plated cells were then
607 exposed to one of four doses of UV radiation: 0, 30, 60, or 90 J/m^2. UV intensity was calibrated
608 using a UVX Radiometer UVP and dosage calculated by varying time of exposure to a short-
609 wave UV transilluminator. After irradiation, plates were grown at 30°C for 2 days in the dark to
610 avoid photoreactivation repair, and then at room temperature for 5 days. Individual colonies
611 were counted and fraction survivals were calculated and plotted.
612
613
614
615
616

617 **REFERENCES**
618

619 1. A. Vannini, P. Cramer, Conservation between the RNA Polymerase I, II, and III
620 Transcription Initiation Machineries. *Molecular Cell* **45**, 439-446 (2012).
621 2. M. C. Thomas, C.-M. Chiang, The general transcription machinery and general cofactors.
622 *Critical reviews in biochemistry and molecular biology* **41**, 105-178 (2006).
623 3. S. Grünberg, L. Warfield, S. Hahn, Architecture of the RNA polymerase II preinitiation
624 complex and mechanism of ATP-dependent promoter opening. *Nature structural &*
625 *molecular biology* **19**, 788-796 (2012).
626 4. S. Schilbach *et al.*, Structures of transcription pre-initiation complex with TFIIH and
627 Mediator. *Nature* **551**, 204-209 (2017).
628 5. P. J. Robinson *et al.*, Structure of a Complete Mediator-RNA Polymerase II Pre-Initiation
629 Complex. *Cell* **166**, 1411-1414.e1416 (2016).
630 6. Y. He *et al.*, Near-atomic resolution visualization of human transcription promoter
631 opening. *Nature* **533**, 359-365 (2016).
632 7. P. Sung, D. Higgins, L. Prakash, S. Prakash, Mutation of lysine-48 to arginine in the yeast
633 RAD3 protein abolishes its ATPase and DNA helicase activities but not the ability to bind
634 ATP. *EMBO J* **7**, 3263-3269 (1988).
635 8. G. S. Winkler *et al.*, TFIIH with inactive XPD helicase functions in transcription initiation
636 but is defective in DNA repair. *J Biol Chem* **275**, 4258-4266 (2000).
637 9. T. van Eeuwen *et al.*, Cryo-EM structure of TFIIH/Rad4-Rad23-Rad33 in damaged DNA
638 opening in nucleotide excision repair. *Nat Commun* **12**, 3338 (2021).
639 10. J. Kim *et al.*, Lesion recognition by XPC, TFIIH and XPA in DNA excision repair. *Nature*
640 **617**, 170-175 (2023).
641 11. J. Yu *et al.*, Dynamic conformational switching underlies TFIIH function in transcription
642 and DNA repair and impacts genetic diseases. *Nat Commun* **14**, 2758 (2023).
643 12. S. Schilbach, H. Wang, C. Dienemann, P. Cramer, Yeast PIC-Mediator structure with RNA
644 polymerase II C-terminal domain. *Proc Natl Acad Sci U S A* **120**, e2220542120 (2023).
645 13. A. C. Schier, D. J. Taatjes, Everything at once: cryo-EM yields remarkable insights into
646 human RNA polymerase II transcription. *Nat Struct Mol Biol* **28**, 540-543 (2021).
647 14. S. Buratowski, Progression through the RNA Polymerase II CTD Cycle. *Molecular Cell* **36**,
648 541-546 (2009).
649 15. R. P. Fisher, D. O. Morgan, A novel cyclin associates with MO15/CDK7 to form the CDK-
650 activating kinase. *Cell* **78**, 713-724 (1994).
651 16. M. J. Cismowski, G. M. Laff, M. J. Solomon, S. I. Reed, KIN28 encodes a C-terminal
652 domain kinase that controls mRNA transcription in Saccharomyces cerevisiae but lacks
653 cyclin-dependent kinase-activating kinase (CAK) activity. *Mol Cell Biol* **15**, 2983-2992
654 (1995).
655 17. F. H. Espinoza, A. Farrell, H. Erdjument-Bromage, P. Tempst, D. O. Morgan, A cyclin-
656 dependent kinase-activating kinase (CAK) in budding yeast unrelated to vertebrate CAK.
657 *Science* **273**, 1714-1717 (1996).
658 18. P. Kaldis, A. Sutton, M. J. Solomon, The Cdk-activating kinase (CAK) from budding yeast.
659 *Cell* **86**, 553-564 (1996).

660 19. S. Peissert, A. Schlosser, R. Kendel, J. Kuper, C. Kisker, Structural basis for CDK7
661 activation by MAT1 and Cyclin H. *Proc Natl Acad Sci U S A* **117**, 26739-26748 (2020).
662 20. B. J. Greber *et al.*, The cryoelectron microscopy structure of the human CDK-activating
663 kinase. *Proc Natl Acad Sci U S A* **117**, 22849-22857 (2020).
664 21. T. van Eeuwen *et al.*, Structure of TFIIK for phosphorylation of CTD of RNA polymerase II.
665 *Sci Adv* **7** (2021).
666 22. L. Warfield, J. Luo, J. Ranish, S. Hahn, Function of Conserved Topological Regions within
667 the Saccharomyces cerevisiae Basal Transcription Factor TFIIH. *Molecular and Cellular*
668 *Biology* **36**, 2464-2475 (2016).
669 23. Y. Chun *et al.*, Selective Kinase Inhibition Shows That Bur1 (Cdk9) Phosphorylates the
670 Rpb1 Linker In Vivo. *Molecular and Cellular Biology* **39**, e00602-00618 (2019).
671 24. E. J. Cho, M. S. Kobor, M. Kim, J. Greenblatt, S. Buratowski, Opposing effects of Ctk1
672 kinase and Fcp1 phosphatase at Ser 2 of the RNA polymerase II C-terminal domain.
673 *Genes and Development* **15**, 3319-3329 (2001).
674 25. K. Glover-Cutter *et al.*, TFIIH-associated Cdk7 kinase functions in phosphorylation of C-
675 terminal domain Ser7 residues, promoter-proximal pausing, and termination by RNA
676 polymerase II. *Molecular and Cellular Biology* **29**, 5455-5464 (2009).
677 26. J. L. Corden, RNA polymerase II C-terminal domain: Tethering transcription to transcript
678 and template. *Chemical reviews* **113**, 8423-8455 (2013).
679 27. D. Eick, M. Geyer, The RNA polymerase II carboxy-terminal domain (CTD) code. *Chemical*
680 *reviews* **113**, 8456-8490 (2013).
681 28. N. Yurko *et al.*, MPK1/SLT2 Links Multiple Stress Responses with Gene Expression in
682 Budding Yeast by Phosphorylating Tyr1 of the RNAP II CTD. *Molecular Cell* **68**, 913-
683 925.e913 (2017).
684 29. W. J. Feaver *et al.*, Subunit interactions in yeast transcription/repair factor TFIIH.
685 Requirement for Tfb3 subunit in nucleotide excision repair. *Journal of Biological*
686 *Chemistry* **275**, 5941-5946 (2000).
687 30. T. Watanabe *et al.*, The carboxy terminus of the small subunit of TFIIE regulates the
688 transition from transcription initiation to elongation by RNA polymerase II. *Molecular*
689 *and Cellular Biology* **23**, 2914-2926 (2003).
690 31. K. H. Wong, Y. Jin, K. Struhl, TFIIH Phosphorylation of the Pol II CTD Stimulates Mediator
691 Dissociation from the Preinitiation Complex and Promoter Escape. *Molecular Cell* **54**,
692 601-612 (2014).
693 32. M. C. Keogh, V. Podolny, S. Buratowski, Bur1 kinase is required for efficient transcription
694 elongation by RNA polymerase II. *Molecular and Cellular Biology* **23**, 7005-7018 (2003).
695 33. K. Murakami *et al.*, Tfb6, a previously unidentified subunit of the general transcription
696 factor TFIIH, facilitates dissociation of Ssl2 helicase after transcription initiation.
697 *Proceedings of the National Academy of Sciences of the United States of America* **109**,
698 4816-4821 (2012).
699 34. C. Yang *et al.*, Structural visualization of de novo transcription initiation by
700 Saccharomyces cerevisiae RNA polymerase II. *Mol Cell* **82**, 660-676 e669 (2022).
701 35. K. Helenius *et al.*, Requirement of TFIIH kinase subunit Mat1 for RNA Pol II C-terminal
702 domain Ser5 phosphorylation, transcription and mRNA turnover. *Nucleic Acids Research*
703 **39**, 5025-5035 (2011).

704 36. M. Sano *et al.*, Menage-a-trois 1 is critical for the transcriptional function of
705 PPARgamma coactivator 1. *Cell Metab* **5**, 129-142 (2007).
706 37. M. C. Keogh, E.-J. Cho, V. Podolny, S. Buratowski, Kin28 is found within TFIIH and a
707 Kin28-Ccl1-Tfb3 trimer complex with differential sensitivities to T-loop phosphorylation.
708 *Molecular and Cellular Biology* **22**, 1288-1297 (2002).
709 38. P. Komarnitsky, E. J. Cho, S. Buratowski, Different phosphorylated forms of RNA
710 polymerase II and associated mRNA processing factors during transcription. *Genes and*
711 *Development* **14**, 2452-2460 (2000).
712 39. H. Suh *et al.*, Direct Analysis of Phosphorylation Sites on the Rpb1 C-Terminal Domain of
713 RNA Polymerase II. *Molecular Cell* **61**, 297-304 (2016).
714 40. J. Abril-Garrido *et al.*, Structural basis of transcription reduction by a promoter-proximal
715 +1 nucleosome. *Mol Cell* **83**, 1798-1809 e1797 (2023).
716 41. X. Chen *et al.*, Structural insights into preinitiation complex assembly on core promoters.
717 *Science* **372** (2021).
718 42. T. M. M. Søgaard, J. Q. Svejstrup, Hyperphosphorylation of the C-terminal repeat
719 domain of RNA polymerase II facilitates dissociation of its complex with mediator.
720 *Journal of Biological Chemistry* **282**, 14113-14120 (2007).
721 43. C. Jeronimo, F. Robert, Kin28 regulates the transient association of Mediator with core
722 promoters. *Nature structural & molecular biology* **21**, 449-455 (2014).
723 44. E. J. Tomko *et al.*, The Role of XPB/Ssl2 dsDNA Translocase Processivity in Transcription
724 Start-site Scanning. *J Mol Biol* **433**, 166813 (2021).
725 45. K. Murakami *et al.*, Uncoupling Promoter Opening from Start-Site Scanning. *Mol Cell* **59**,
726 133-138 (2015).
727 46. J. H. Lee, H. S. Jung, A. Günzl, Transcriptionally active TFIIH of the early-diverged
728 eukaryote Trypanosoma brucei harbors two novel core subunits but not a cyclin-
729 activating kinase complex. *Nucleic Acids Research* **37**, 3811-3820 (2009).
730 47. J. H. Lee *et al.*, A TFIIH-Associated Mediator Head Is a Basal Factor of Small Nuclear
731 Spliced Leader RNA Gene Transcription in Early-Diverged Trypanosomes. *Molecular and*
732 *Cellular Biology* **30**, 5502-5513 (2010).
733 48. N. Badjatia, D. L. Ambrosio, J. H. Lee, A. Gunzl, Trypanosome cdc2-related kinase 9
734 controls spliced leader RNA cap4 methylation and phosphorylation of RNA polymerase II
735 subunit RPB1. *Mol Cell Biol* **33**, 1965-1975 (2013).
736 49. A. Das, V. Bellofatto, The non-canonical CTD of RNAP-II is essential for productive RNA
737 synthesis in Trypanosoma brucei. *PLoS One* **4**, e6959 (2009).
738 50. P. Matsui, J. DePaulo, S. Buratowski, An interaction between the Tfb1 and Ssl1 subunits
739 of yeast TFIIH correlates with DNA repair activity. *Nucleic Acids Research* **23**, 767-772
740 (1995).
741 51. N. H. Kuldell, S. Buratowski, Genetic analysis of the large subunit of yeast transcription
742 factor IIE reveals two regions with distinct functions. *Molecular and Cellular Biology* **17**,
743 5288-5298 (1997).
744 52. R. D. Chapman *et al.*, Transcribing RNA polymerase II is phosphorylated at CTD residue
745 serine-7. *Science (New York, NY)* **318**, 1780-1782 (2007).
746 53. E. Harlow, D. P. Lane, *Antibodies: A Laboratory Manual* (Cold Spring Harbor Laboratory
747 Press, Inc., 1988).

748 54. V. V. Kushnirov, Rapid and reliable protein extraction from yeast. *Yeast* **16**, 857-860
749 (2000).
750 55. C. Jeronimo *et al.*, FACT is recruited to the +1 nucleosome of transcribed genes and
751 spreads in a Chd1-dependent manner. *Mol Cell* 10.1016/j.molcel.2021.07.010 (2021).
752 56. C. Jeronimo, C. Poitras, F. Robert, Histone Recycling by FACT and Spt6 during
753 Transcription Prevents the Scrambling of Histone Modifications. *Cell reports* **28**, 1206-
754 1218.e1208 (2019).
755 57. A. M. Bolger, M. Lohse, B. Usadel, Trimmomatic: a flexible trimmer for Illumina
756 sequence data. *Bioinformatics* **30**, 2114-2120 (2014).
757 58. B. Langmead, C. Trapnell, M. Pop, S. L. Salzberg, Ultrafast and memory-efficient
758 alignment of short DNA sequences to the human genome. *Genome biology* **10**, R25
759 (2009).
760 59. H. Li *et al.*, The Sequence Alignment/Map format and SAMtools. *Bioinformatics (Oxford,*
761 *England)* **25**, 2078-2079 (2009).
762 60. A. R. Quinlan, I. M. Hall, BEDTools: a flexible suite of utilities for comparing genomic
763 features. *Bioinformatics* **26**, 841-842 (2010).
764 61. F. Ramirez *et al.*, deepTools2: a next generation web server for deep-sequencing data
765 analysis. *Nucleic Acids Res* **44**, W160-165 (2016).
766 62. J. Casper *et al.*, The UCSC Genome Browser database: 2018 update. *Nucleic Acids Res* **46**,
767 D762-D769 (2018).
768 63. M. Brunelle *et al.*, Aggregate and Heatmap Representations of Genome-Wide
769 Localization Data Using VAP, a Versatile Aggregate Profiler. *Methods Mol Biol* **1334**, 273-
770 298 (2015).
771 64. C. Coulombe *et al.*, VAP: a versatile aggregate profiler for efficient genome-wide data
772 representation and discovery. *Nucleic Acids Res* **42**, W485-493 (2014).
773 65. V. Pelechano, W. Wei, L. M. Steinmetz, Extensive transcriptional heterogeneity revealed
774 by isoform profiling. *Nature* **497**, 127-131 (2013).
775
776

Figure Legends

Fig. 1. Tfb3 N-term-Linker fusions to other kinase modules can replace Tfb3, but not Kin28. **(A)** Schematic of TFIIH structure within the PIC. The domain structure of Tfb3 (green) is shown, connecting the TFIIH Kinase (cyan) and Core (blue) Modules. **(B)** Schematic of Tfb3 fusions to other kinase modules. (**C)** The *kin28Δ* strain YSB744 was transformed with pRS425 (Vector), pRS415-*KIN28*, pRS425-*TFB3-BUR2*, pRS425-*TFB3-CTK3*, or pRS425-*TFB3-MPK1*. Transformants were tested for the ability to replace a *KIN28/URA3* construct by plasmid shuffling. Cells were streaked on -LEU-TRP (center) or -LEU-TRP+5-FOA (right) plates for 3 days at 30℃. **(D)** pRS315 (Vector), pRS425-*TFB3*, pRS315/TFB3Δ2 (aa 1-275) (29), pRS425-*TFB3-BUR2*, pRS425-*TFB3-CTK3*, and pRS425-*TFB3-MPK1* were transformed into *tfb3Δ* strain SHY907 (22), replacing the plasmid-expressed wild-type gene by plasmid shuffling. Streaks shown were grown on –LEU for 4 days (center) or on -LEU+5-FOA plates (right) for 9 days.

Fig. 2. Tfb3 can be split into two functional parts.
(A) Schematic of Tfb3 deletion constructs. Note that all constructs retained amino acids 1-11 at the N-terminus for ease of cloning and to avoid differential sensitivity to N-end rule degradation. **(B)** Plasmid shuffling was used to test pRS424 (Vector), pRS424-*TFB3* (WT *TFB3*), pRS424-*TFB3(*Δ145-321) (N-term), and pRS424-*TFB3* (Δ252-321) (N-term-Linker) for the ability to support growth of *tfb3Δ* shuffling strain SHY907/YF2456 (22). Streaks shown were grown on -TRP+5-FOA plates for 5 days at 30℃ **(C)** Spot assay for growth. Tfb3 N-term (YSB3704) and N-term-Linker (YSB3722) strains were transformed with pRS425 (Vector), pSH1542 (WT *TFB3*), pRS315-TFB3(1-11, 238-Stop)-Flag1-TAP (C-term low copy), pRS425-TFB3(1-11, 238-Stop) (C-term high copy), pRS425-TFB3(1-11, 139-Stop), or pLH366 (Linker-C-term high copy). Ten-fold serial dilutions were spotted onto –LEU-TRP plates for 3 days. For comparison to normal growth, an isogenic strain carrying WT *TFB3* (YSB3788) was spotted in parallel (top strip).

Fig. 3. The TFIIH Kinase Module associates with the untethered Tfb3 C-terminal domain. (A) Whole cell extracts were made from YSB3788 (*TFB3* untagged), YSB3723 (*TFB3*-TAP + N-term), YSB3732 (N-term-Linker + C-term-TAP), and YSB3728 (N-term + Linker-C-term-TAP). Both Input extracts (lanes 1-4) and IgG-Agarose precipitated fractions (lanes 5-8) were resolved by SDS-PAGE and blotting for Tfb3. **(B)** To probe for other Kinase Module subunits, IgG precipitates were probed with anti-Ccl1 and anti-Kin28 antibodies. In all panels, asterisks mark TAP-tagged Tfb3 derivatives (which also react with secondary antibody due to the protein A component).

Fig. 4. Splitting Tfb3 uncouples the TFIIH Kinase Module from the Core Module and the PIC. The same IgG-Agarose precipitates analyzed in **Fig. 3** were also probed with the following antibodies against: **(A)** TFIIH Core Module subunit Tfb1 (note background binding of Tfb1 to beads as seen in lane 1, and non-specific band ~50 kDa), and **(B)** TFIIE subunits Tfa1 and Tfa2 (note non-specific band ~60 kDa), which serves as a marker for the RNApII PIC. In all panels, asterisks mark TAP-tagged Tfb3 derivatives reacting with secondary antibody due to the protein A component.

820 **Figure 5**. **Loss of proper Kinase Module and Ser5P promoter localization in split Tfb3 cells**.
821 Crosslinked chromatin was prepared from strains expressing full length Tfb3 (YSB3788), the
822 separated N-term-Linker and C-term derivatives (YSB3731), the N-term and Linker-C-term
823 derivatives (YSB3727), or N-term and C-term with no Linker (YSB3725). Samples were
824 immunoprecipitated and processed for sequencing of crosslinked DNA as described in
825 Methods. Two biological replicates for each antibody were used to generate metagene profiles
826 of **(A)** TFIIH Core subunit Tfb1, **(B)** TFIIH Kinase subunit Kin28, **(C)** Rpb1 CTD Ser5P, **(D)** RNApII
827 subunit Rpb1, and **(E)** Ser5P normalized to total Rpb1. The analysis used only those nuclear
828 genes with an average RNApII occupancy greater than 4 reads per million (rpm) and longer than
829 1 kb (n=95). Individual replicates are shown in **Supplemental Fig. S3**. To account for the
830 differing lengths of genes, each graph shows 1 kb centered on the transcription start site (TSS)
831 to the left of the dividing line, and 1 kb centered on the polyadenylation site (pA) to the right.
832
833 **Figure 6**. **Split Tfb3 strains are not hyper-sensitive to UV light**. Yeast strains carrying the
834 indicated Tfb3 configurations were plated at various densities and exposed to the indicated
835 dosages of UV light. Surviving colonies were counted after several days. The graph shows the
836 averaged values from multiple replicates, and error bars represent standard deviation. Note
837 that there are two strain backgrounds. The *tfb1-101* strain (YSB250, black) is a positive control
838 for an NER-defective strain sensitive to UV light, and its isogenic WT control is YSB207 (yellow).
839 The other five isogenic strains are in a *tfb6Δ* background, lacking the Tfb6 protein that
840 competes with the TFIIH for Ssl2 binding (33): WT/tfb6Δ (YSB3788, green), N-term (YSB3724,
841 red), N-term-Linker (YSB3729, blue), N-term + Linker-C-term (YSB3727, orange), and N-term-
842 Linker + C-term (YSB3731, slate).
843
844 **Figure 7. Model for linkage between the TFIIH Kinase and Core Module functions. A.** In free
845 TFIIH, the Tfb3 linker contacts the Ssl2/XPB subunit to create a "closed" conformation. In this
846 configuration, the translocase, and possibly the kinase, may be inhibited. **B.** Upon TFIIH
847 incorporation as the final component of the PIC, the Kinase Module engages with both
848 Mediator (not pictured) and the CTD. These interactions may help release the Tfb3/MAT1 linker
849 from Ssl2/XPB, allowing the translocase to access downstream DNA to promote ATP hydrolysis
850 and promoter melting.
851
852
853

Fig. 1

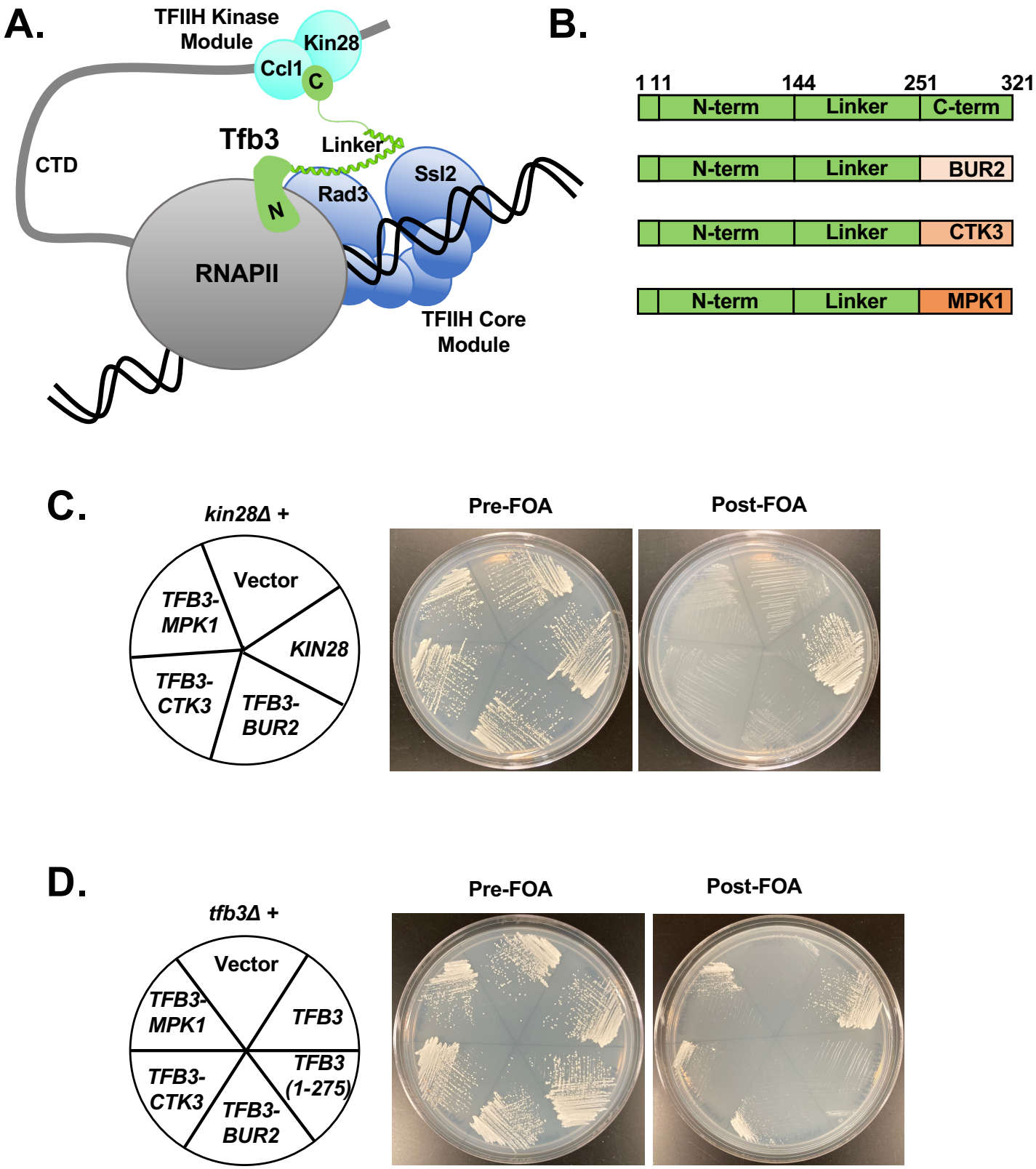
A.
TFIIH Kinase Module
Kin28
Ccl1
C
CTD
Tfb3
Linker
N
Rad3
Ssl2
RNAPII
TFIIH Core Module
B.
1 11
144
251
321
N-term
Linker
C-term
N-term
Linker
BUR2
N-term
Linker
CTK3
N-term
Linker
MPK1
C.
kin28Δ +
Vector
TFB3-MPK1
KIN28
TFB3-CTK3
TFB3-BUR2
Pre-FOA
Post-FOA
D.
tfb3Δ +
Vector
TFB3-MPK1
TFB3
TFB3-CTK3
TFB3 (1-275)
TFB3-BUR2
Pre-FOA
Post-FOA

Fig. 2

A.

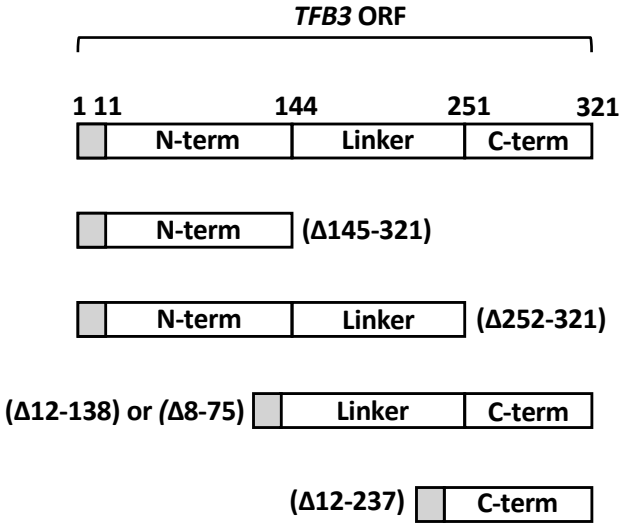
TFB3 ORF
1 11
144
251
321
N-term
Linker
C-term
N-term
(Δ145-321)
N-term
Linker
(Δ252-321)
(Δ12-138) or (Δ8-75)
Linker
C-term
(Δ12-237)
C-term

B.

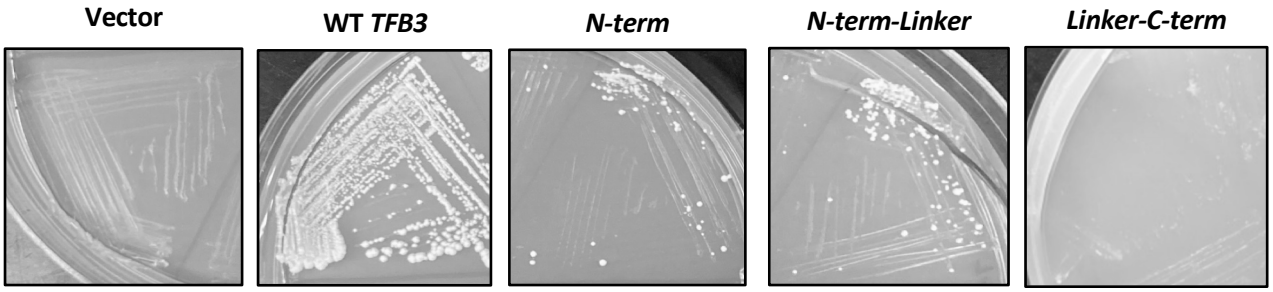
Vector
WT TFB3
N-term
N-term-Linker
Linker-C-term

C.

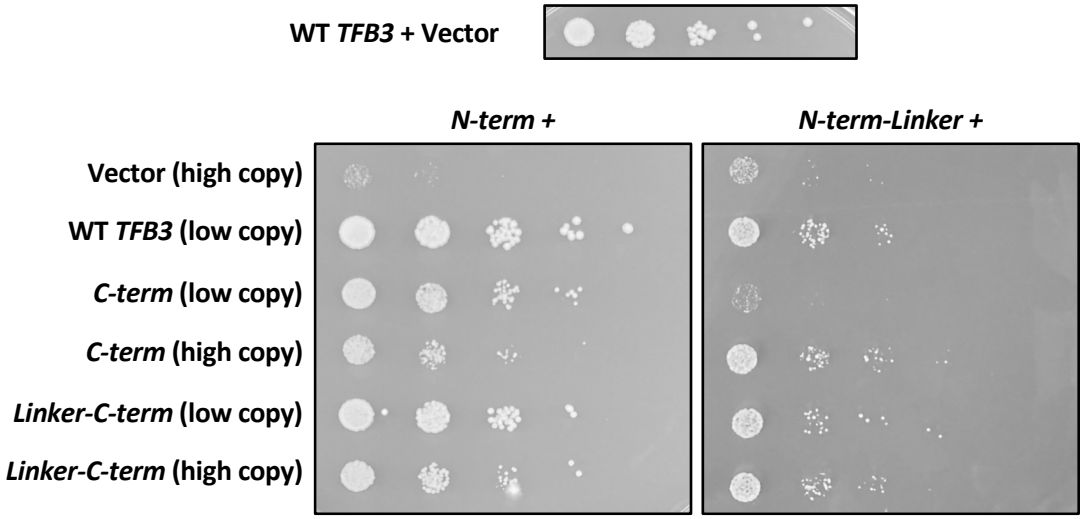
WT TFB3 + Vector
N-term +
N-term-Linker +
Vector (high copy)
WT TFB3 (low copy)
C-term (low copy)
C-term (high copy)
Linker-C-term (low copy)
Linker-C-term (high copy)

Fig. 3

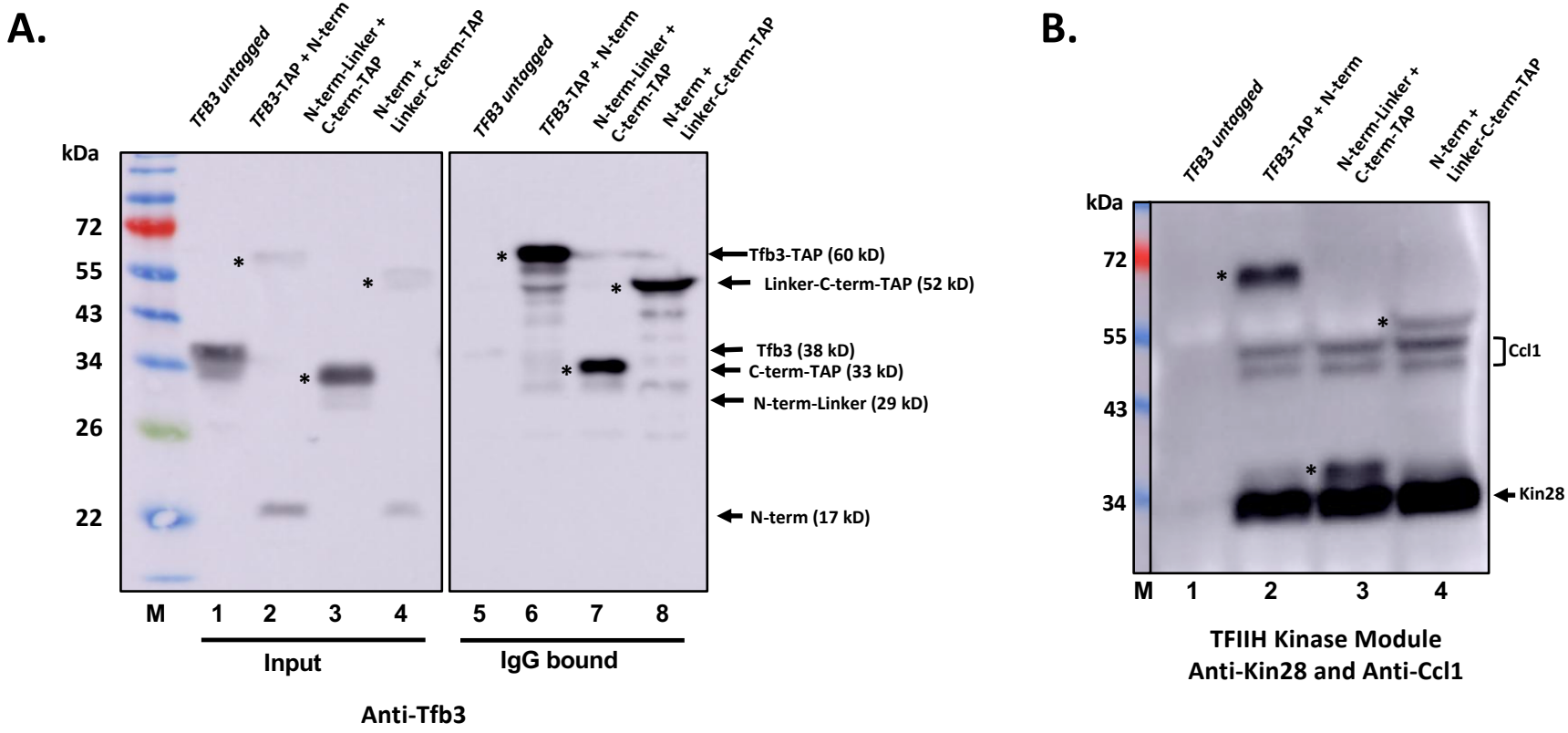
A.
TFB3 untagged
TFB3-TAP + N-term
N-term-Linker + C-term-TAP
N-term + Linker-C-term-TAP
kDa
72
55
43
34
26
22
Tfb3-TAP (60 kD)
Linker-C-term-TAP (52 kD)
Tfb3 (38 kD)
C-term-TAP (33 kD)
N-term-Linker (29 kD)
N-term (17 kD)
M 1 2 3 4 5 6 7 8
Input
IgG bound
Anti-Tfb3
B.
TFB3 untagged
TFB3-TAP + N-term
N-term-Linker + C-term-TAP
N-term + Linker-C-term-TAP
kDa
72
55
43
34
Ccl1
Kin28
M 1 2 3 4
TFIIH Kinase Module
Anti-Kin28 and Anti-Ccl1

Fig. 4

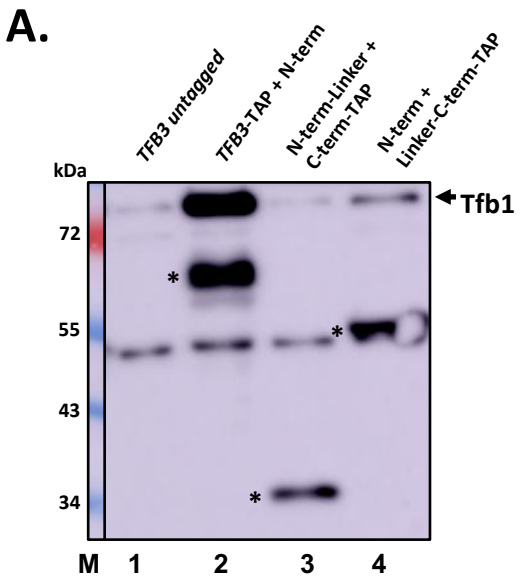

TFIIH Core Module
Anti-Tfb1

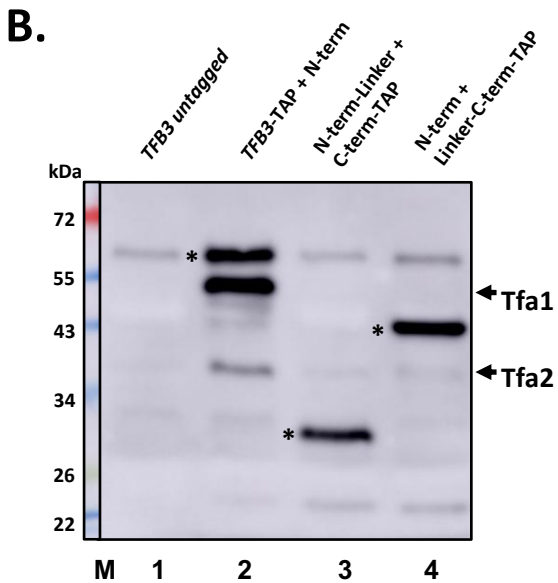

TFIIE
Anti-Tfa1 and Anti-Tfa2

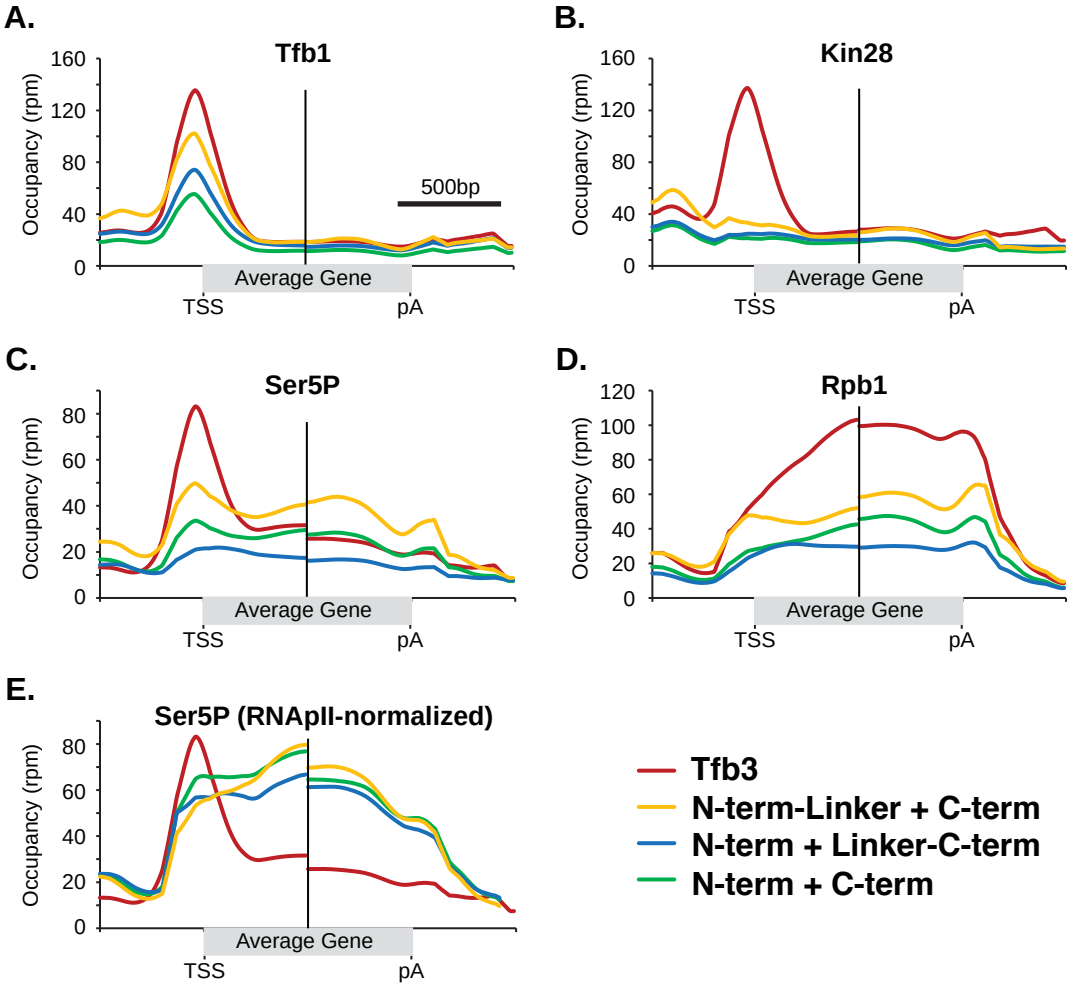
A.
Tfb1
Occupancy (rpm)
160
120
80
40
0
500bp
Average Gene
TSS
pA
B.
Kin28
Occupancy (rpm)
160
120
80
40
0
Average Gene
TSS
pA
C.
Ser5P
Occupancy (rpm)
80
60
40
20
0
Average Gene
TSS
pA
D.
Rpb1
Occupancy (rpm)
120
100
80
60
40
20
0
Average Gene
TSS
pA
E.
Ser5P (RNApII-normalized)
Occupancy (rpm)
80
60
40
20
0
Average Gene
TSS
pA
Tfb3
N-term-Linker + C-term
N-term + Linker-C-term
N-term + C-term

Fig 5

Fig. 6

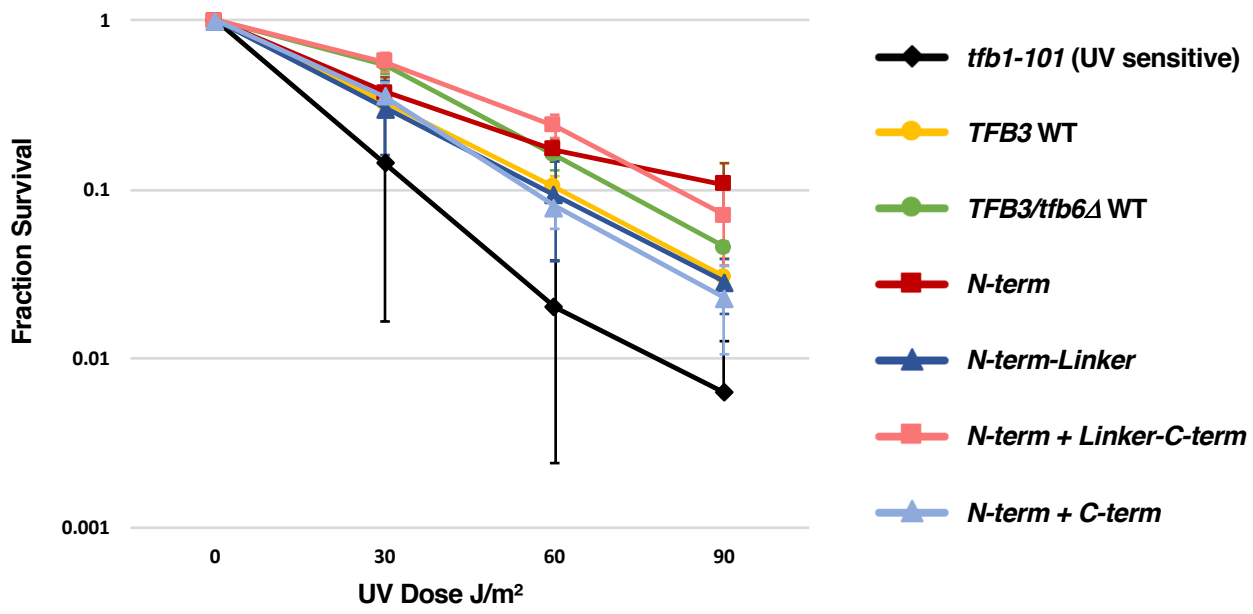
1
0.1
0.01
0.001
Fraction Survival
0
30
60
90
UV Dose J/m²
tfb1-101 (UV sensitive)
TFB3 WT
TFB3/tfb6Δ WT
N-term
N-term-Linker
N-term + Linker-C-term
N-term + C-term

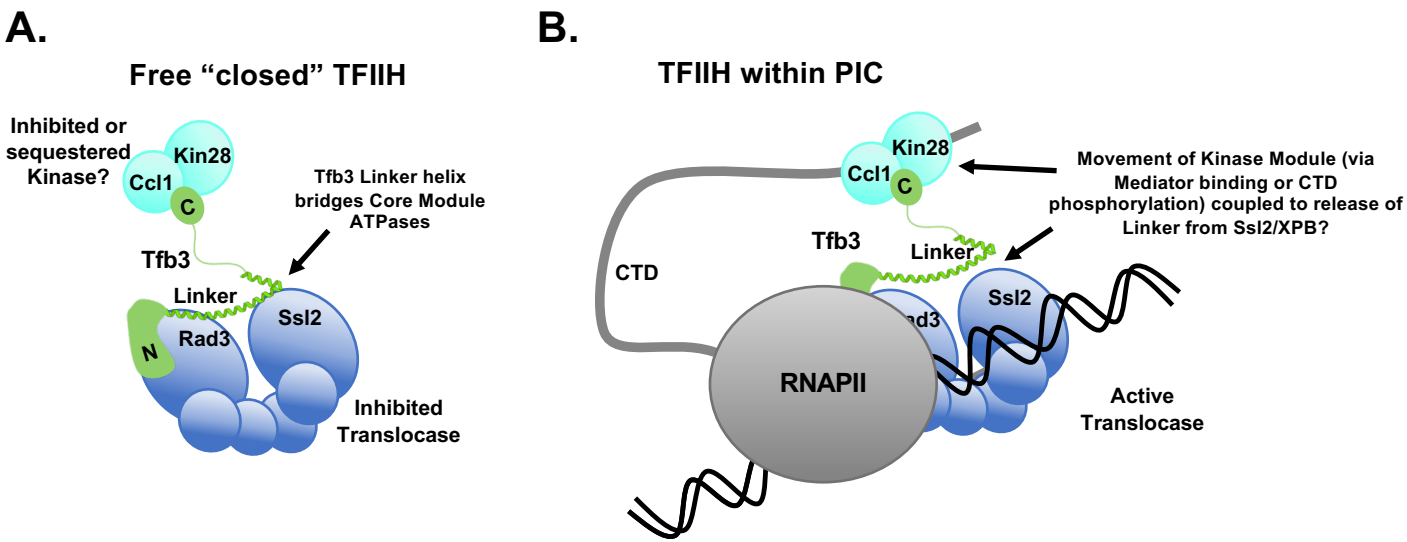
A.
Free "closed" TFIIH
Inhibited or sequestered Kinase?
Kin28
Ccl1
C
Tfb3 Linker helix bridges Core Module ATPases
Tfb3
Linker
Ssl2
Rad3
N
Inhibited Translocase
B.
TFIIH within PIC
Kin28
Ccl1
C
Movement of Kinase Module (via Mediator binding or CTD phosphorylation) coupled to release of Linker from Ssl2/XPB?
Tfb3
Linker
CTD
Ssl2
RNAPII
Active Translocase